Supporting Information

Macrometallocycle Binuclear NHC Silver(I): Synthesis, Structure and Recognition for *o*-Phenylenediamine

Qing-Xiang Liu*, Deng-Che Wei, Dong-Xue Zhao, Xiao-Feng Sun, Zhi-Xiang Zhao and Jing Yan

Table of Contents

1. CCDC numbers for complexes 1-4.

CCDC 1408696-1408699 contains the supplementary crystallographic data for complexes **1-4**. These data can be obtained free of charge via http//www.ccdc.cam.ac.uk/conts/retrieving.html, or from the Cambridge Crystallographic Data Centre, 12 Union Road, Cambridge, CB2 1EZ, UK; fax: (+44) 1223-336-033; or e-mail: deposit@ccdc.cam.ac.uk.

2. The dihedral angles of complexes 1-4.

Table S1. The dihedral angles (˚) between two benzimidazole (or imidazole) rings in the same NHC-Ag-NHC unit (**A**), the dihedral angles (˚) between two benzimidazole (or imidazole) rings in the same ligand (**B**), the dihedral angles (˚) between benzimidazole (or imidazole) rings and anthraquinone ring in the same ligand (**C**), the dihedral angles (˚) between two anthraquinone rings in each molecule (**D**) and the dihedral angles (˚) between benzimidazole (or imidazole) rings and adjacent benzene rings (**E**) for complexes **1-4**.

Compounds	**A**	**B**	**C**	**D**	**E**
1	23.5(5) 23.5(5)	23.5(5) 23.5(5)	70.4(6), 73.8(6) 88.4(8), 78.6(3)	15.2(8)	89.2(8), 71.4(9)
2	22.7(3) 22.7(2)	22.7(3) 22.7(3)	76.5(4), 79.0(3) 79.7(3), 74.1(4)	26.9(5)	88.4(5), 87.9(3) 88.3(5), 74.7(4)
3	36.4(3) 50.2(3)	45.5(3) 45.5(4)	9.3(9), 47.6(3) 7.6(5), 48.5(6)	10.0(5)	81.8(1), 77.5(9) 66.4(4), 76.4(5)
4	59.6(2) 59.3(3)	39.1(3) 29.4(2)	46.1(3), 42.8(3) 56.9(3), 53.3(4)	38.6(2)	68.3(3), 87.6(4) 86.3(5), 71.2(3)

3. The distances (Å) of Ag ···Ag and π-π interactions for 1-4.

Table S2. The distances (Å) of Ag ···Ag and π-π interactions for **1-4**.

Complexes	Ag ···Ag	π-π	
		face-to-face	center-to-center
1	11.048(9)	3.463(1) (anthraquinone and anthraquinone); 3.378(1) (anthraquinone and benzimidazole)	3.662(7) (anthraquinone and anthraquinone); 3.561(2) (anthraquinone and benzimidazole)
2	12.141(5)	3.625(2) (anthraquinone and anthraquinone); 3.551(6) (anthraquinone and benzene)	3.747(8) (anthraquinone and anthraquinone); 3.755(1) (anthraquinone and benzene)
3	11.537(1)	3.221(2) and 3.577(1) (anthraquinone and benzimidazole)	3.453(6) and 3.666(0) (anthraquinone and benzimidazole)
4	11.507(1)	3.315(2) and 3.391(2) (anthraquinone and imidazole)	3.473(4) and 3.706 (7) (anthraquinone and imidazole)

4. H-Bonding geometry of complexes 1-4.

Table S3. H-Bonding Geometry (Å, °) for **1-4**.

	D-H ···A	D-H	H ···A	D ···A	D-H ···A
1	C(2)-H(2) ··F(3)^{ii}	0.950(2)	2.654(6)	3.565(8)	160.7(3)
	C(78)-H(78B) ··F(1)^{iii}	0.980(2)	2.415(6)	3.347(8)	158.7(3)
2	C(32)-H(32A) ··F(6)^{ii}	0.970	2.585(5)	3.193(7)	120.8(3)
	C(30)-H(30) ··F(4)^{iii}	0.930	2.323(4)	3.227(6)	163.8(3)
	C(31)-H(31) ··F(6)^{iii}	0.930	2.456(6)	3.173(3)	133.9(3)
	C(21)-H(21) ··F(4)^{iv}	0.929	2.608(4)	3.192(5)	121.3(2)
	C(10)-H(10) ··F(2)^{v}	0.929	2.425(6)	3.239(7)	146.2(3)
3	C(6)-H(6A) ··F(9)^{i}	0.949(7)	3.188(9)	3.491(1)	100.6(4)
	C(86)-H(86) ··F(7)^{ii}	0.951(6)	2.456(1)	3.346(1)	155.5(4)
	C(45)-H(45) ··F(11)^{ii}	0.948(7)	2.723(1)	3.494(1)	138.8(5)
	C(54)-H(54) ··F(11)^{ii}	0.950(1)	3.286(1)	3.519(1)	96.2(7)
	C(59)-H(59) ··F(9)^{ii}	0.950(1)	3.094(9)	3.867(1)	139.5(1)

4	C(43)-H(43) ··F(3)^{i}	0.930	2.756(9)	3.734(3)	165.9(2)
	C(52)-H(52B) ··F(6)^{ii}	0.969	2.736(5)	3.449(7)	130.8(3)
	C(12)-H(12B) ··F(1)^{iii}	0.970	2.776(9)	3.734(3)	165.9(2)
	C(77)-H(77) ··F(5)^{iv}	0.970	2.849(9)	3.474(3)	124.3(1)
	C(4)-H(4) ··F(12)^{ii}	0.930	2.739(7)	3.516(1)	141.5(4)
	C(62)-H(62) ··F(12)^{v}	0.930	2.997(7)	3.722(1)	135.9(5)

Symmetry code: ii: -2 + *x*, 2 + *y*, *z*, iii: -2 + *x*, 2 + *y*, -1 + *z* for **1**; ii: 0.5 + *x*, 1.5 - *y*, -0.5 + *z* , iii: -*x*, 1 - *y*, 1 - *z* for **2**; i = *x*, *y*, *z*, ii: 1 - *x*, 1 - *y*, 1 - *z* for **3**; i = -2 + *x*, 0.5 - *y*, -0.5 + *z*, ii: -1 - *x*, 0.5 + *y*, 1.5 - *z*, iii = -2 + *x*, 1+ *y*, *z*, iv = -2 + *x*, *y*, *z* for **4**.

5. The crystal packings of complexes 1-4.

2D supramolecular layer of **1** (Fig. S1) is formed through C-H ··F hydrogen bonds[S1] and intermolecular π-π interactions[S2] from anthraquinone rings and benzimidazole rings with the face-to-face separation of 3.378(1) Å (the center-to-center separation being 3.561(2) Å). In C-H ··F hydrogen bonds, the hydrogen atoms are from methylene and benzyl groups (the data of hydrogen bonds being given in Table S3).

In the crystal packing of **2** (Fig. S2), 2D supramolecular layer is formed through C-H ··F hydrogen bonds and intermolecular π-π interactions between anthraquinone rings and benzene rings with the face-to-face separation of 3.551(6) Å (the center-to-center separation being 3.755(1) Å). In the hydrogen bonds, the hydrogen atoms are from methylene groups, anthraquinone rings and imidazole rings.

In the crystal packing of **3** (Fig. S3), 2D supramolecular layer is formed through C-H ··F hydrogen bonds. In the hydrogen bonds, the hydrogen atoms are from the benzyl groups and benzimidazole groups.

In the crystal packing of **4** (Fig. S4), 2D supramolecular layer is formed through C-H ··F hydrogen bonds. In the hydrogen bonds, the hydrogen atoms are from methylene groups and benzyl groups.

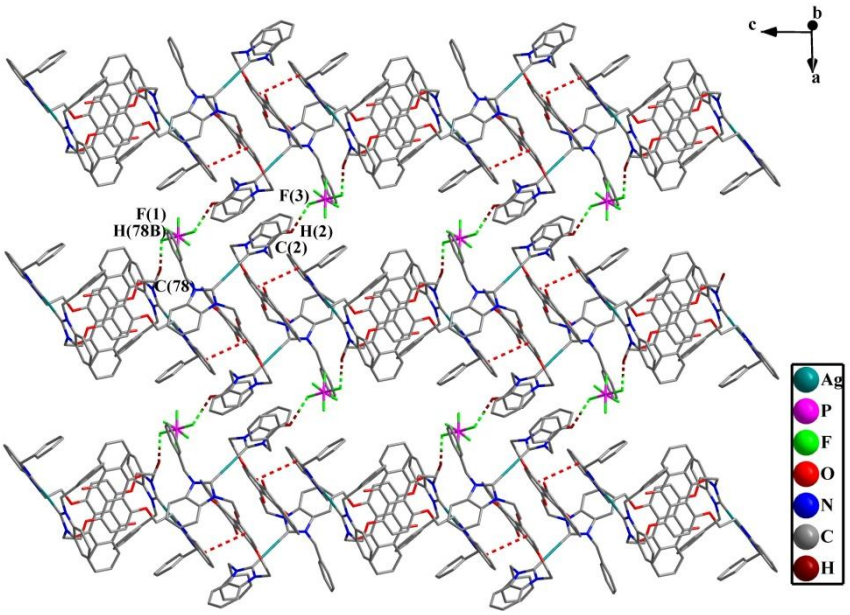

Fig. S1 2D supramolecular layer of **1** via C-H···F hydrogen bonds and π-π interactions. All hydrogen atoms except those participating in C-H···F hydrogen bonds were omitted for clarity.

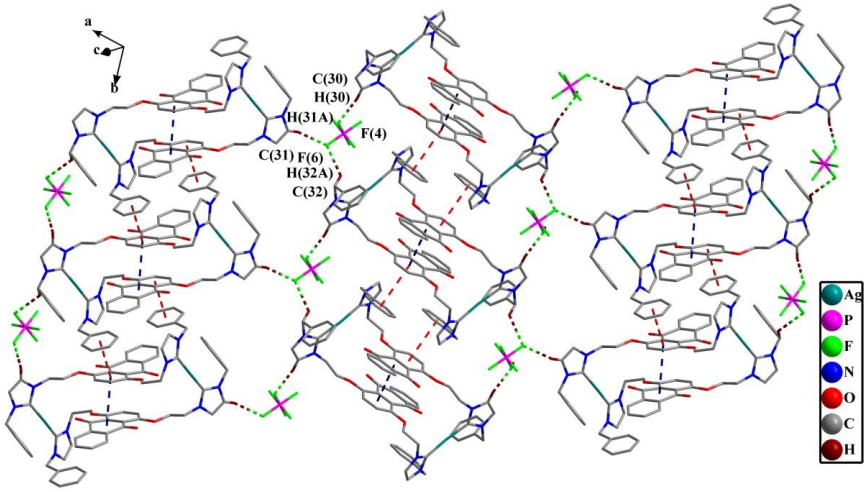

Fig. S2 2D supramolecular layer of **2** via C-H···F hydrogen bonds and π-π interactions. All hydrogen atoms except those participating in C-H···F hydrogen bonds were omitted for clarity.

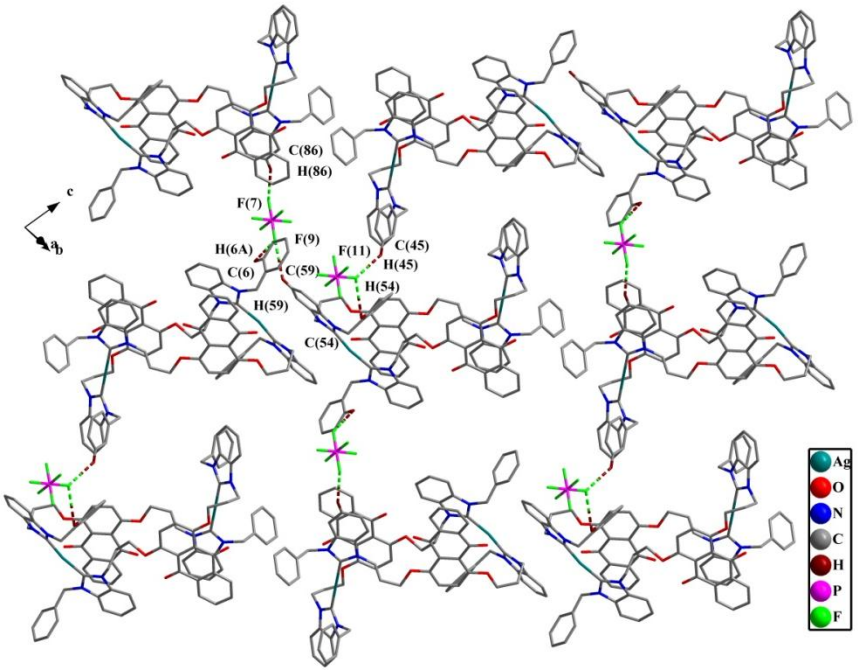

Fig. S3 2D supramolecular layer of **3** via C-H ··F hydrogen bonds. All hydrogen atoms except those participating in C-H ··F hydrogen bonds were omitted for clarity.

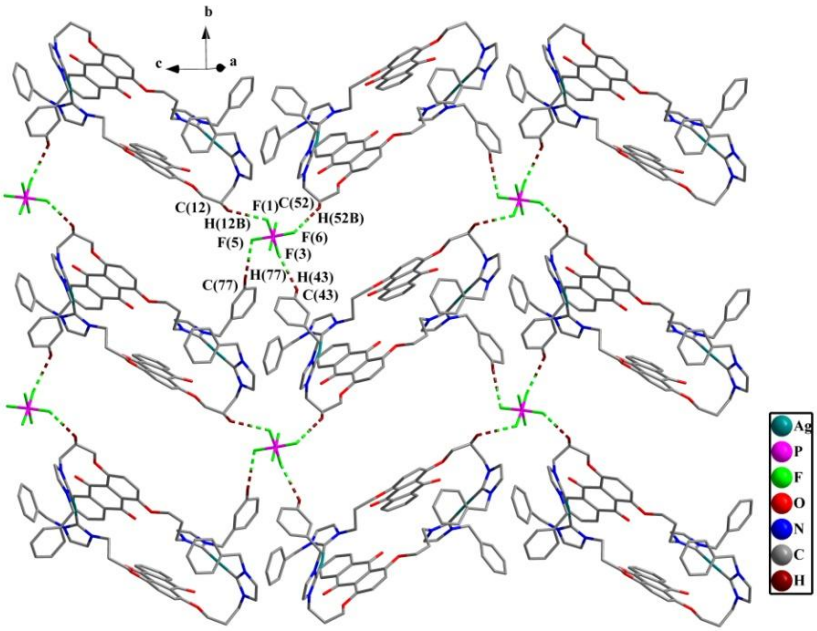

Fig. S4 2D supramolecular layer of **4** via C-H ··F hydrogen bonds. All hydrogen atoms except those participating in C-H ··F hydrogen bonds were omitted for clarity.

References

S1 W. Wei, M. Y. Wu, Y. G. Huang, Q. Gao, F. L. Jiang and M. C. Hong, *Z. Anorg. Allg. Chem.*, 2008, **634**, 2623-2628.

S2 A. L. Pickering, G. Seeber, D. L. Long and L. Cronin, *CrystEngComm.*, 2005, **7**, 504-510.

6. The fluorescence and UV/vis studies of complex 4.

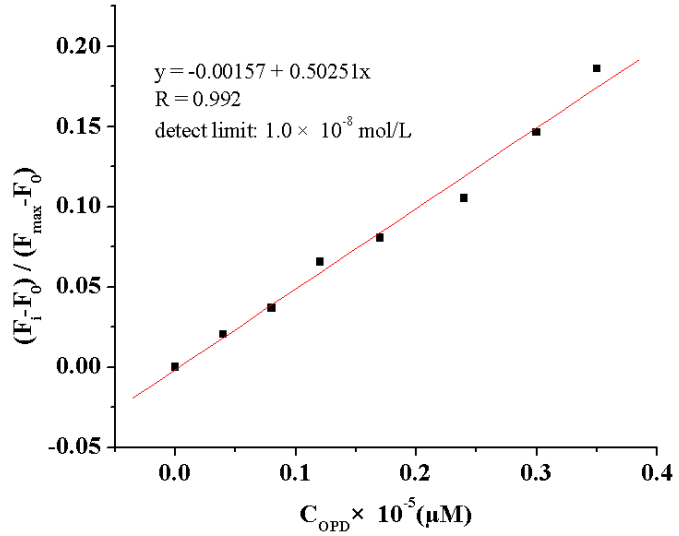

Fig. S5 Emission (at 539 nm) of **4** at different concentrations of *o*-phenylenediamine (0, 0.04, 0.08, 0.12, 0.17, 0.24, 0.30, 0.35 μM) added, normalized between the minimum emission (0.0 μM *o*-phenylenediamine) and the emission (0.35 μM *o*-phenylenediamine). The detection limit was determined to be 1.0×10^{-8} mol/L.

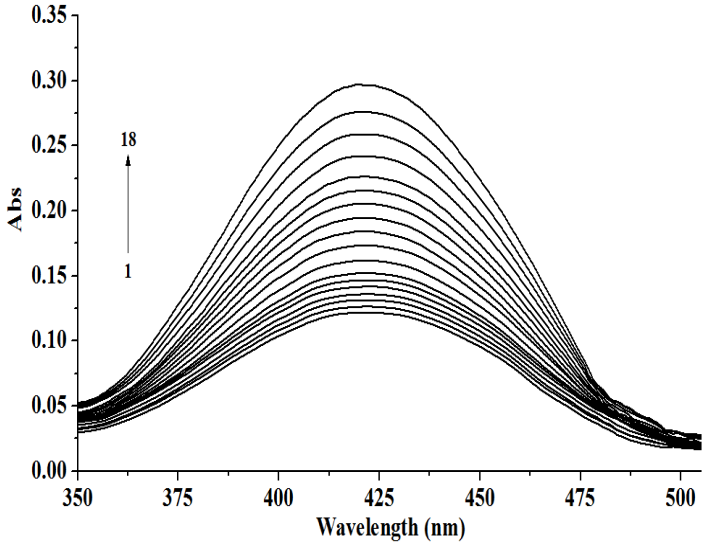

Fig. S6 UV/vis absorption spectra of **4** (1.0×10^{-5} mol/L) in the presence of different concentrations of *o*-phenylenediamine in CH_3OH at 25 ˚C. The concentrations of

o-phenylenediamine for curves 1-18 (from bottom to top) are: 0, 0.025, 0.05, 0.075, 0.1, 0.125, 0.15, 0.2, 0.25, 0.3, 0.35, 0.4, 0.45, 0.5, 0.6, 0.725, 0.85, 1.0 × 10^{-5} mol/L.

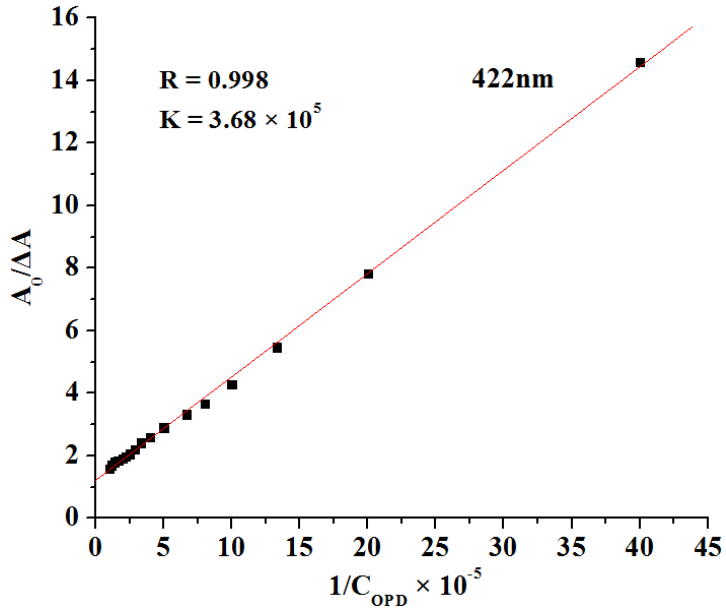

Fig. S7 Benesi-Hildebrand plot of **4** (1.0 × 10^{-5} mol/L)) in the presence of *o*-phenylenediamine in CH_3OH at 422 nm at 25˚C. C_{OPD} is 0, 0.025, 0.05, 0.075, 0.1, 0.125, 0.15, 0.2, 0.25, 0.3, 0.35, 0.4, 0.45, 0.5, 0.6, 0.725, 0.85, 1.0 × 10^{-5} mol/L.

7. HRMS spectra of 4 OPD.

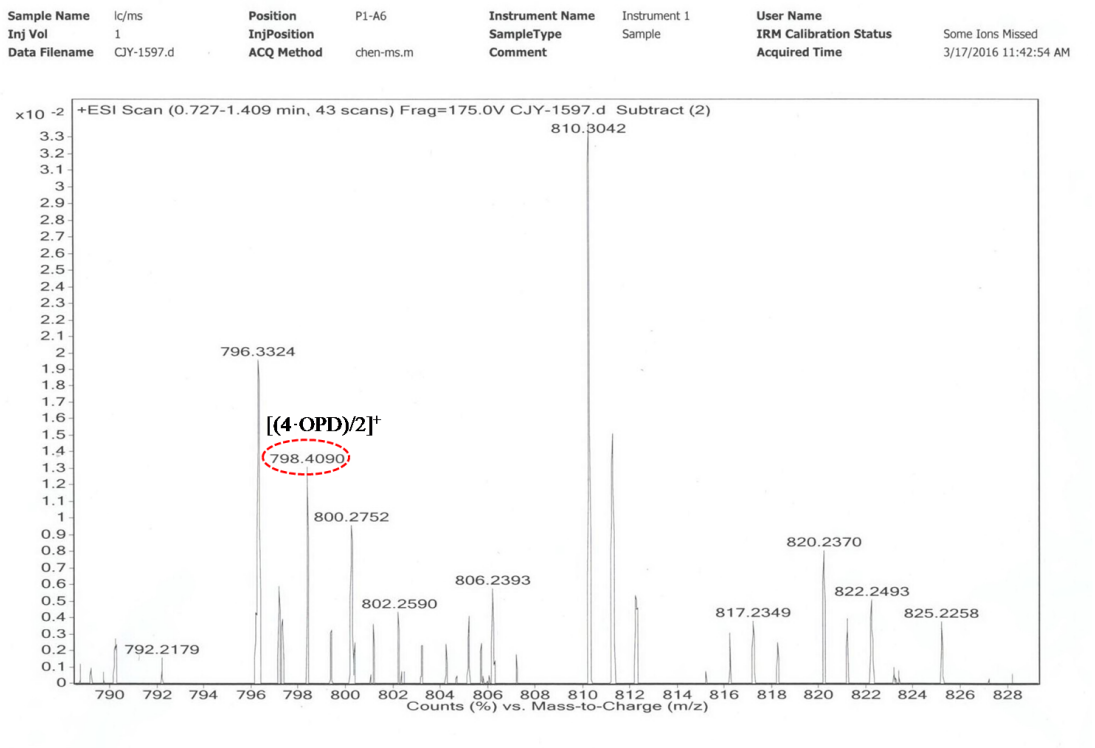

Fig. S8 HRMS spectrum of **4** OPD. MS (EI): m/z [(**4** OPD)/2]$^{+}$ = 798.4090.

8. IR spectra of 4, OPD and 4 ·OPD.

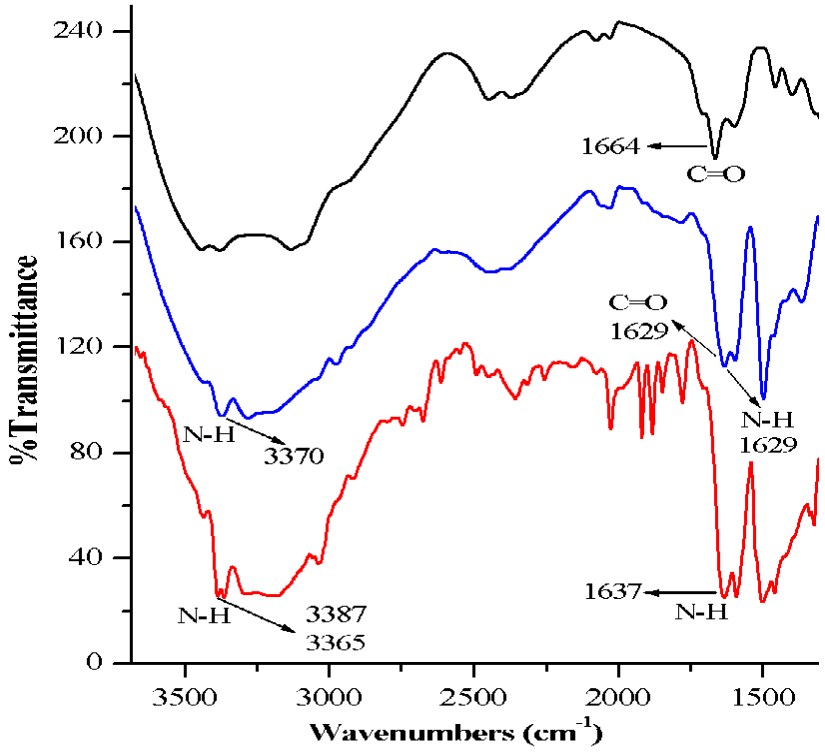

Fig. S9 Infrared spectroscopy of complex **4** (top), **4** ·OPD (middle) and OPD (bottom).

9. The ^{1}H NMR and ^{13}C NMR spectra of precursors $L^{1}H_2(PF_6)_2$-$L^{4}H_2(PF_6)_2$ and complexes 1-4.

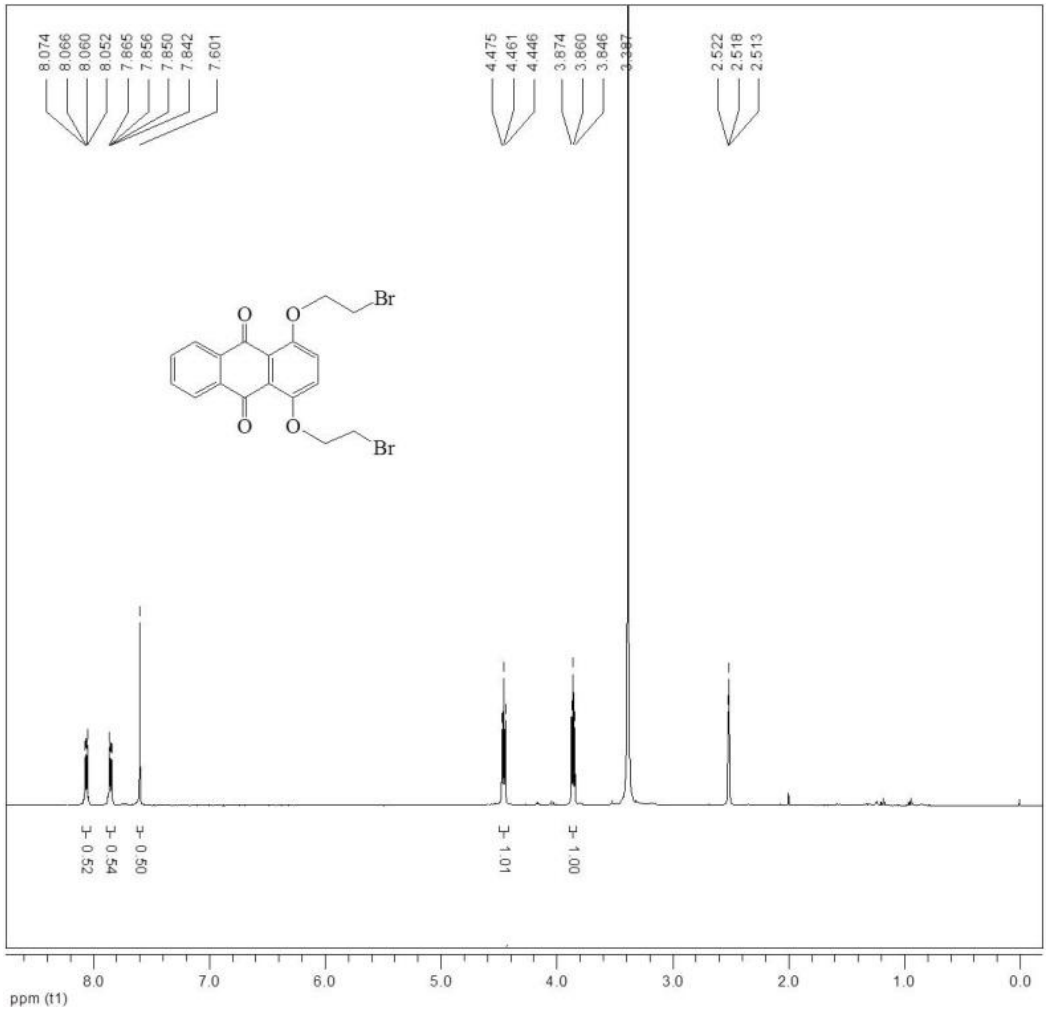

Fig. S10 The ^{1}H NMR (400 MHz, DMSO-d_6) spectrum of 1,4-bis(2'-bromoethoxy)-9,10-anthraquinone.

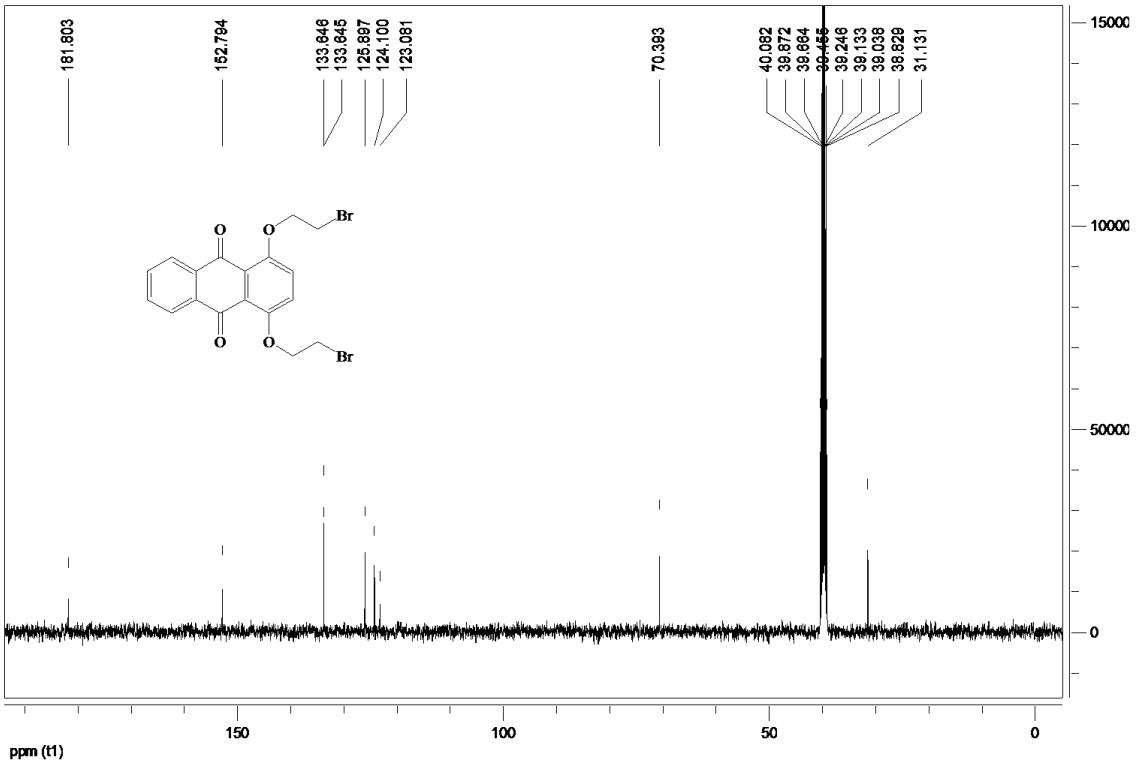

Fig. S11 The ^{13}C NMR (100 MHz, DMSO-d_6) spectrum of 1,4-bis(2'-bromoethoxy)-9,10-anthraquinone.

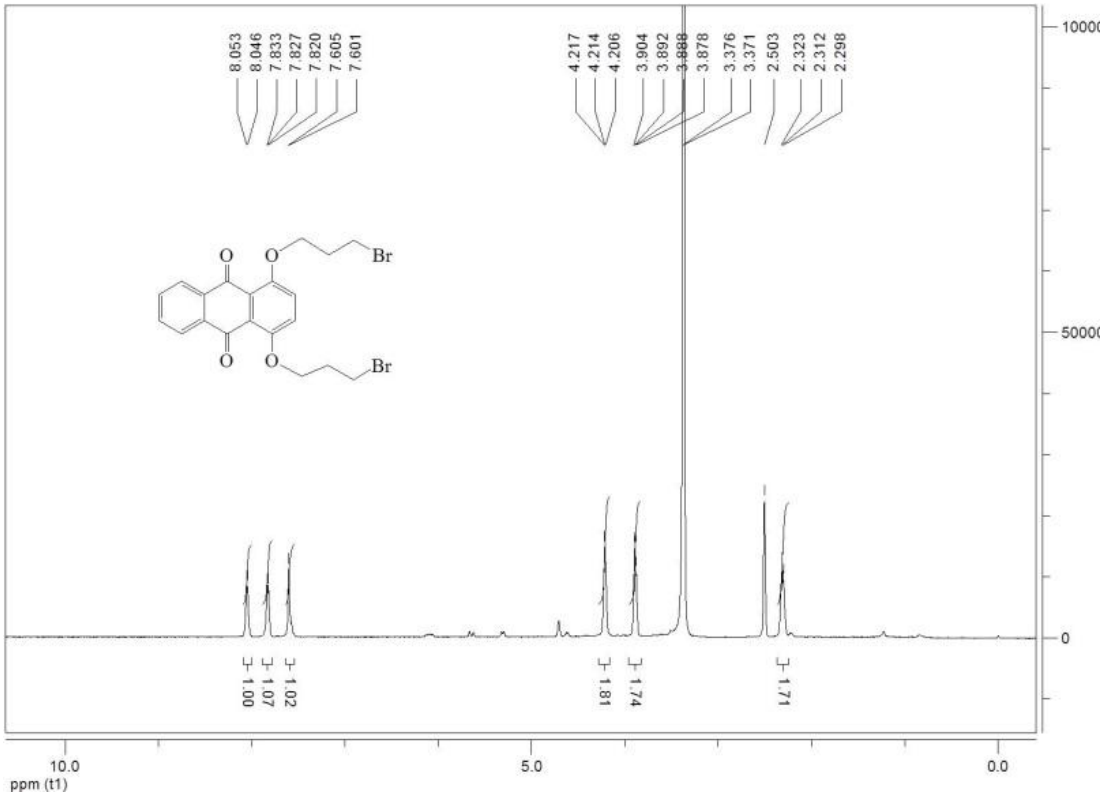

Fig. S12 The ^{1}H NMR (400 MHz, DMSO-d_6) spectrum of 1,4-bis(3'-bromopropoxy)-9,10-anthraquinone.

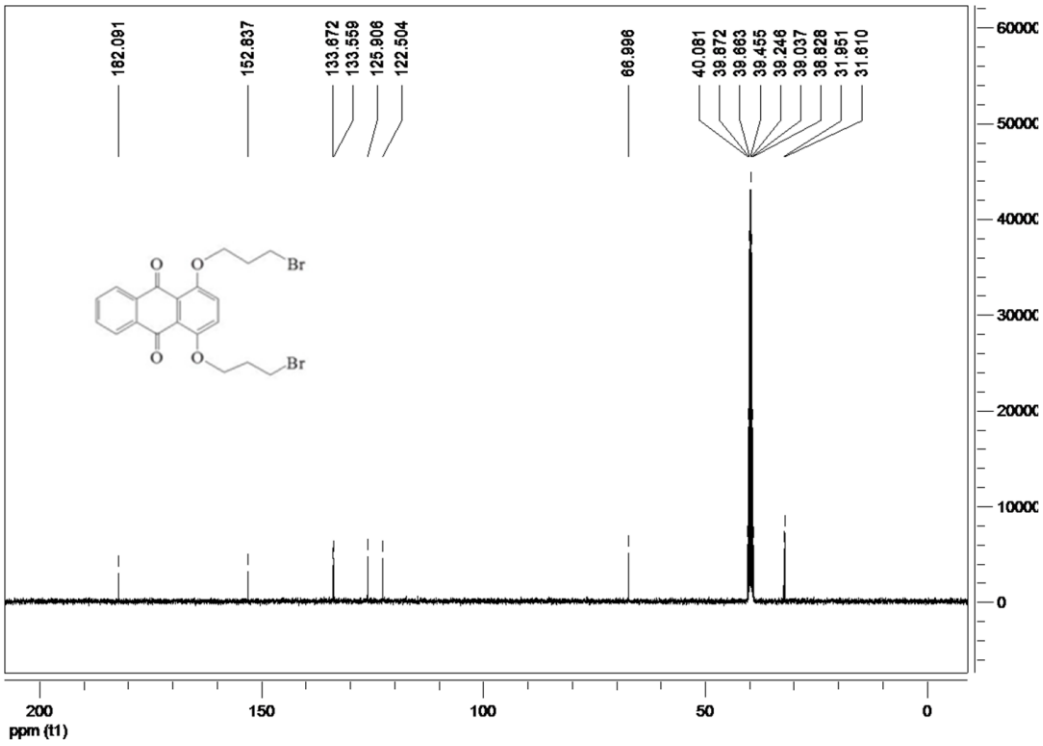

Fig. S13 The ^{13}C NMR (100 MHz, DMSO-d_6) spectrum of 1,4-bis(3'-bromopropoxy)-9,10-anthraquinone.

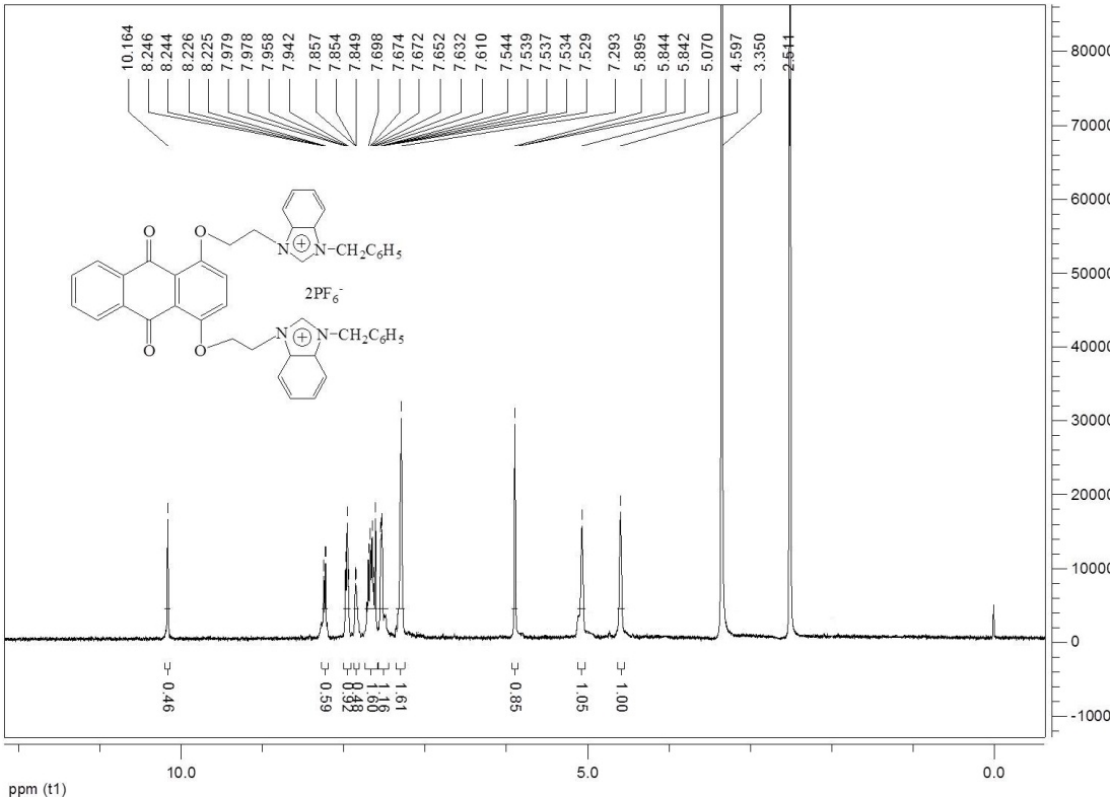

Fig. S14 The ^{1}H NMR (400 MHz, DMSO-d_6) spectrum of $\mathbf{L^1H_2\ (PF_6)_2}$.

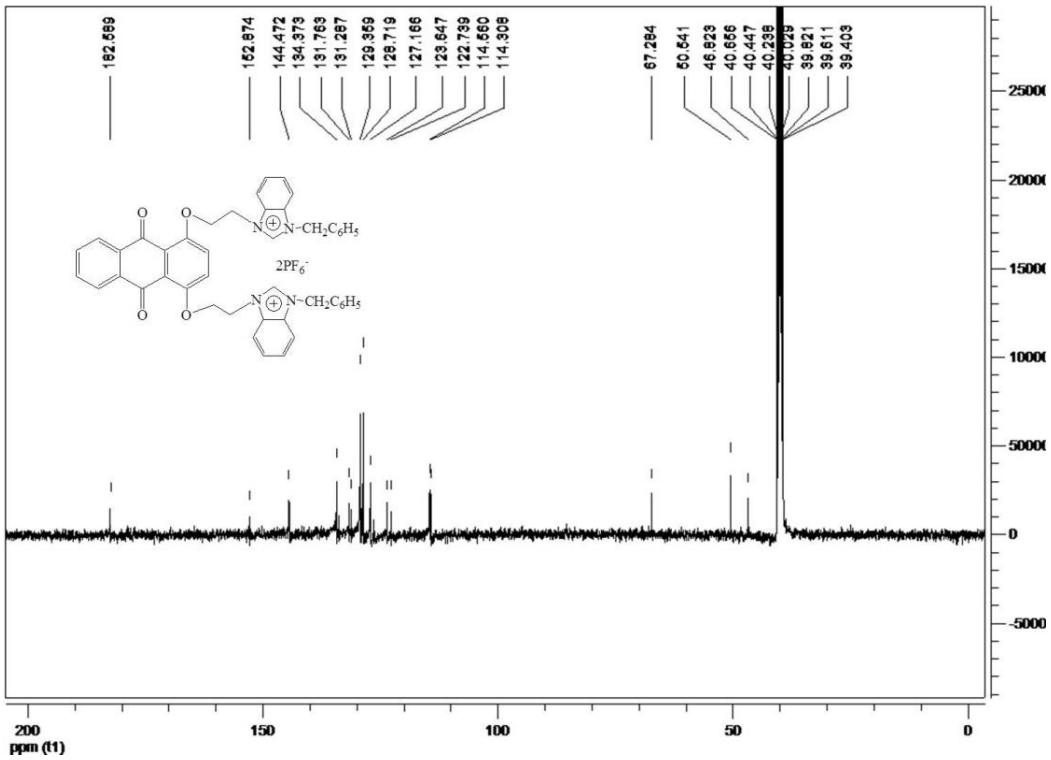

Fig. S15 The ^{13}C NMR (100 MHz, DMSO-d_6) spectrum of $\mathbf{L^1H_2\ (PF_6)_2}$.

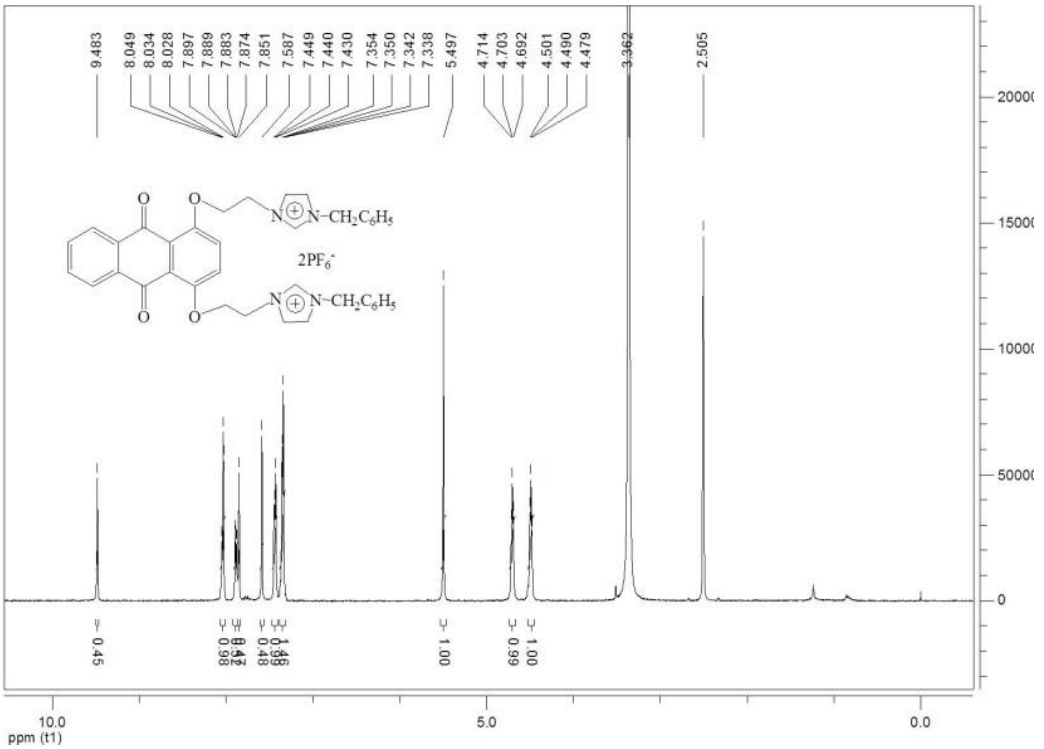

Fig. S16 The ^{1}H NMR (400 MHz, DMSO-d_6) spectrum of $\mathbf{L^2H_2\ (PF_6)_2}$.

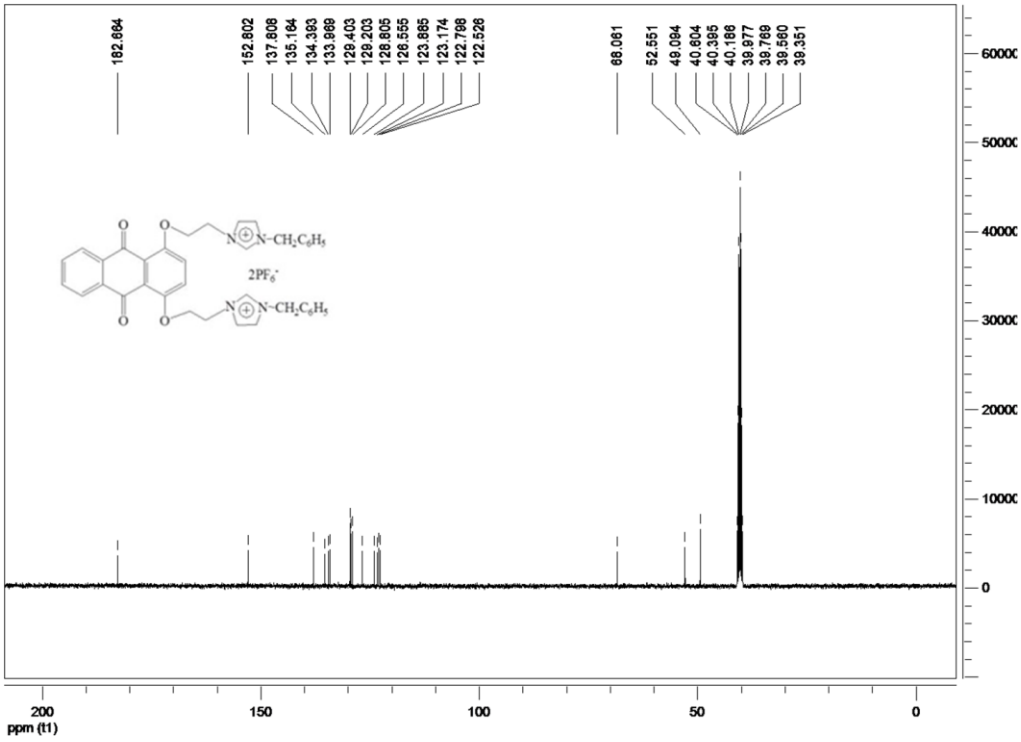

Fig. S17 The ^{13}C NMR (100 MHz, DMSO-d_6) spectrum of $\mathbf{L^2H_2\ (PF_6)_2}$.

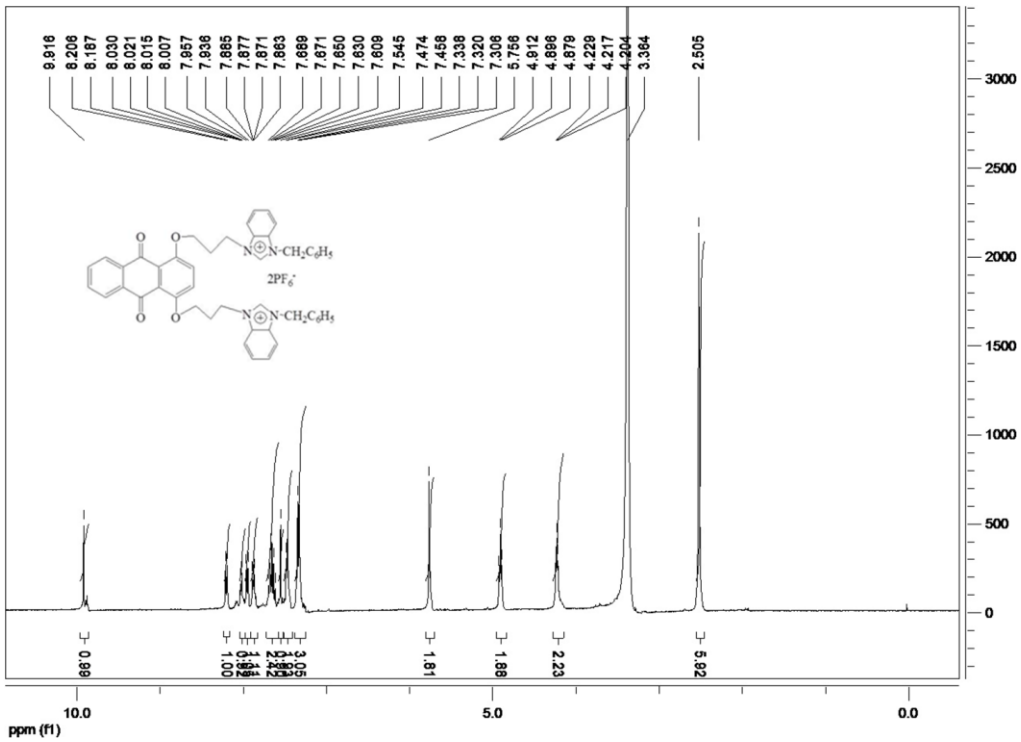

Fig. S18 The ^{1}H NMR (400 MHz, DMSO-d_6) spectrum of $\mathbf{L^3H_2\ (PF_6)_2}$.

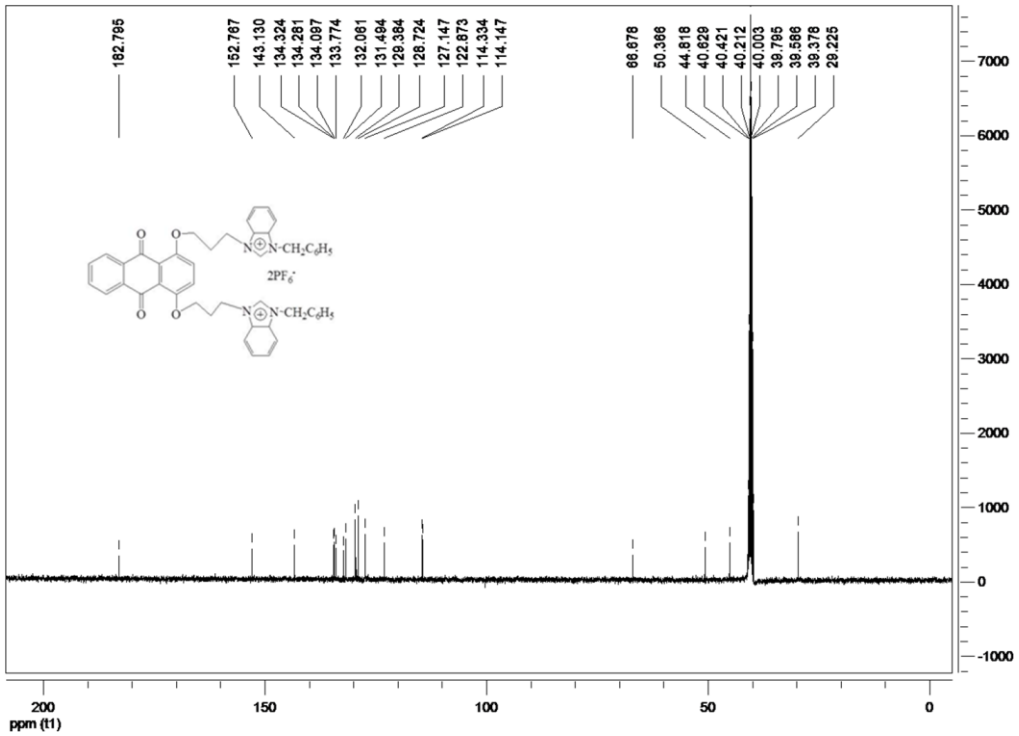

Fig. S19 The ^{13}C NMR (100 MHz, DMSO-d_6) spectrum of $\mathbf{L^3H_2\ (PF_6)_2}$.

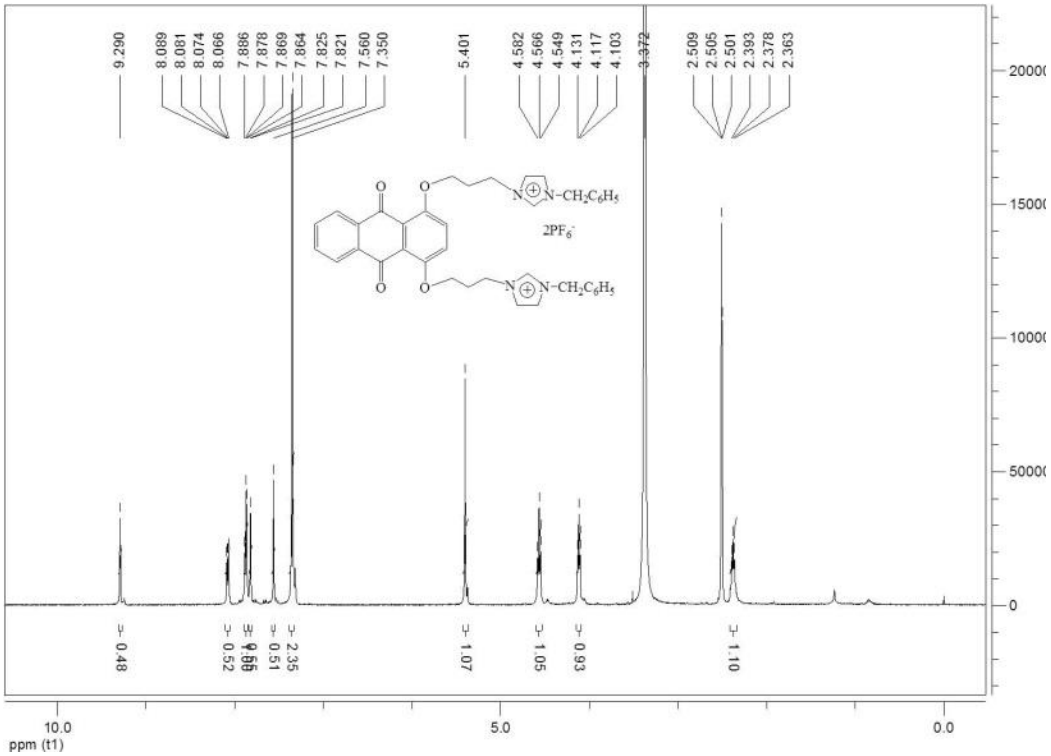

Fig. S20 The ^{1}H NMR (400 MHz, DMSO-d_6) spectrum of $\mathbf{L^4H_2\ (PF_6)_2}$.

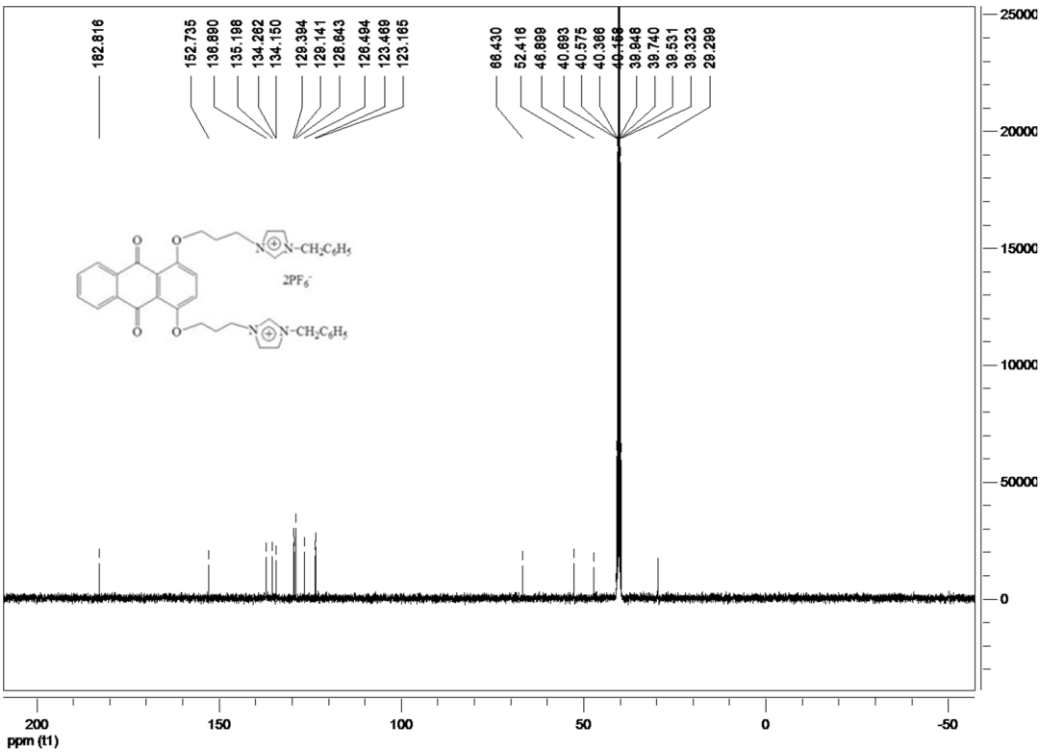

Fig. S21 The ^{13}C NMR (100 MHz, DMSO-d_6) spectrum of $\mathbf{L^4H_2\ (PF_6)_2}$.

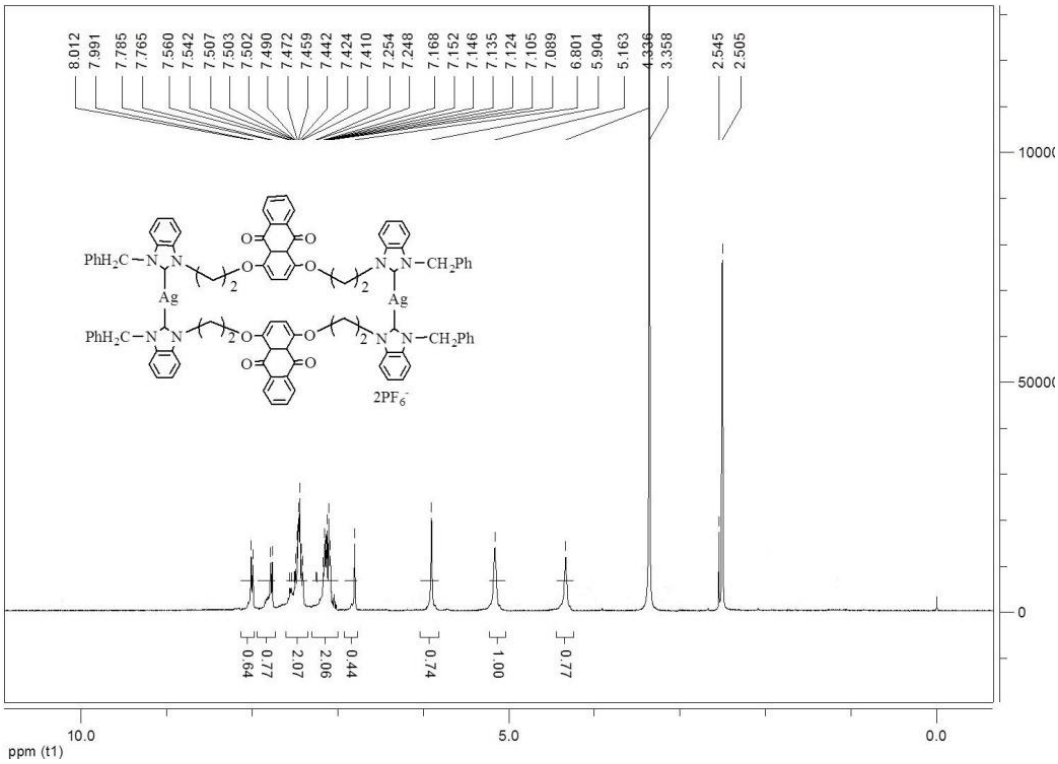

Fig. S22 The ^{1}H NMR (400 MHz, DMSO-d_6) spectrum of complex **1**.

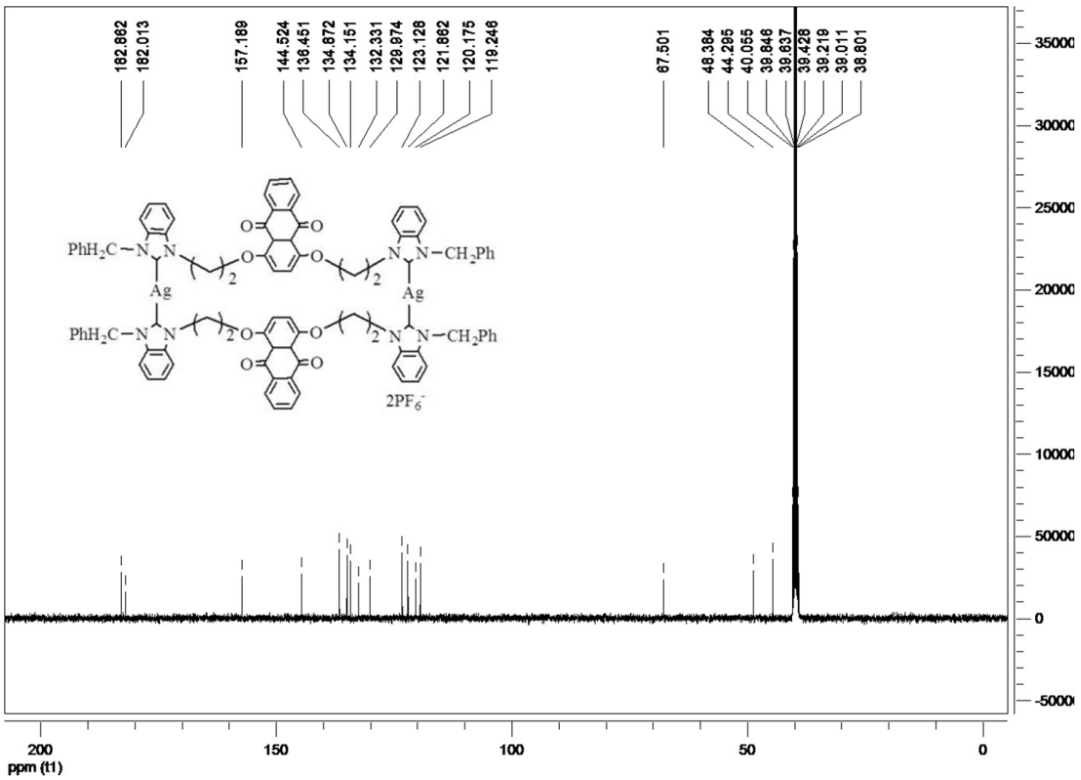

Fig. S23 The ^{13}C NMR (100 MHz, DMSO-d_6) spectrum of complex **1**.

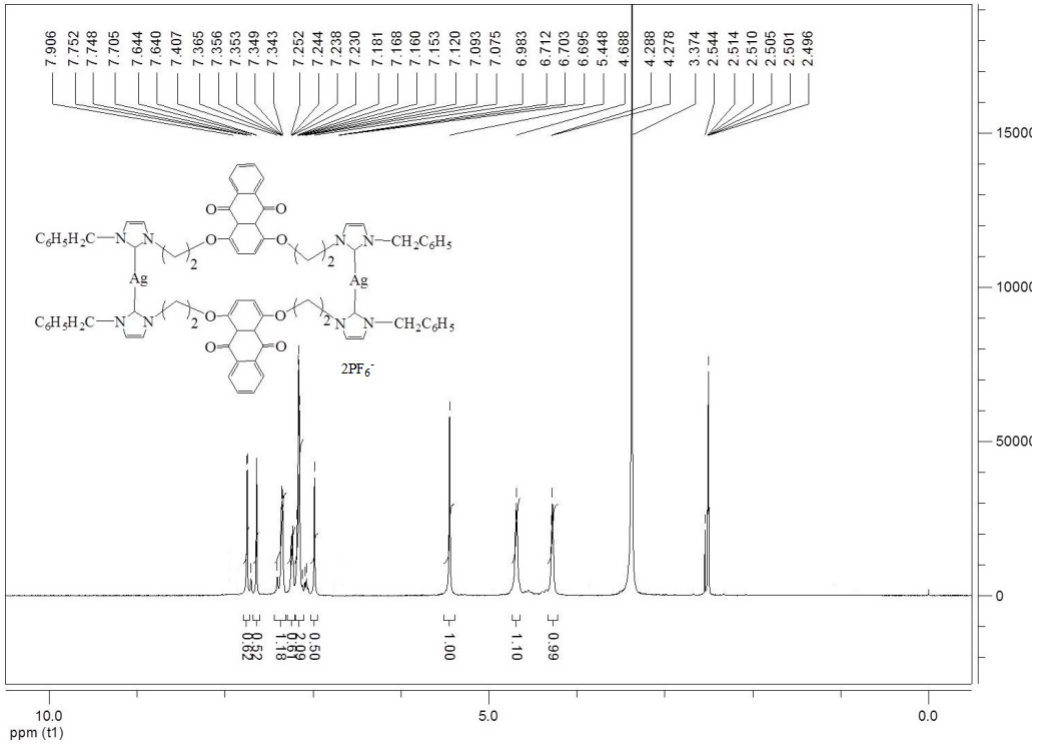

Fig. S24 The ^{1}H NMR (400 MHz, DMSO-d_6) spectrum of complex **2**.

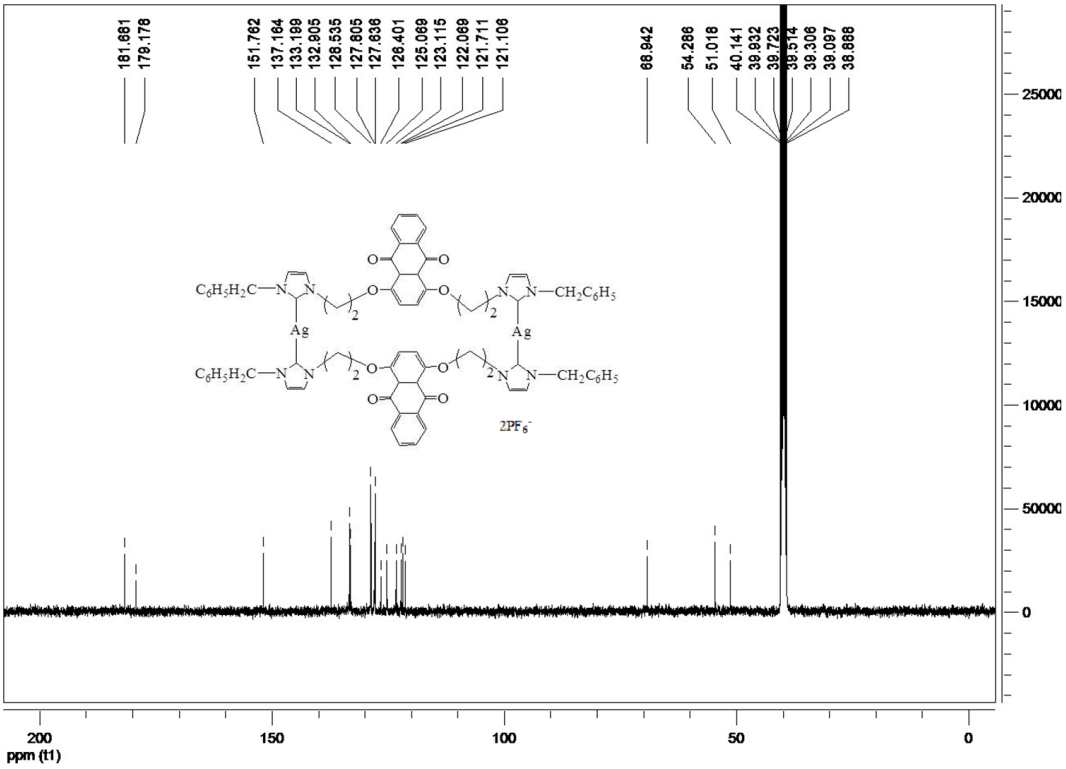

Fig. S25 The ^{13}C NMR (100 MHz, DMSO-d_6) spectrum of complex **2**.

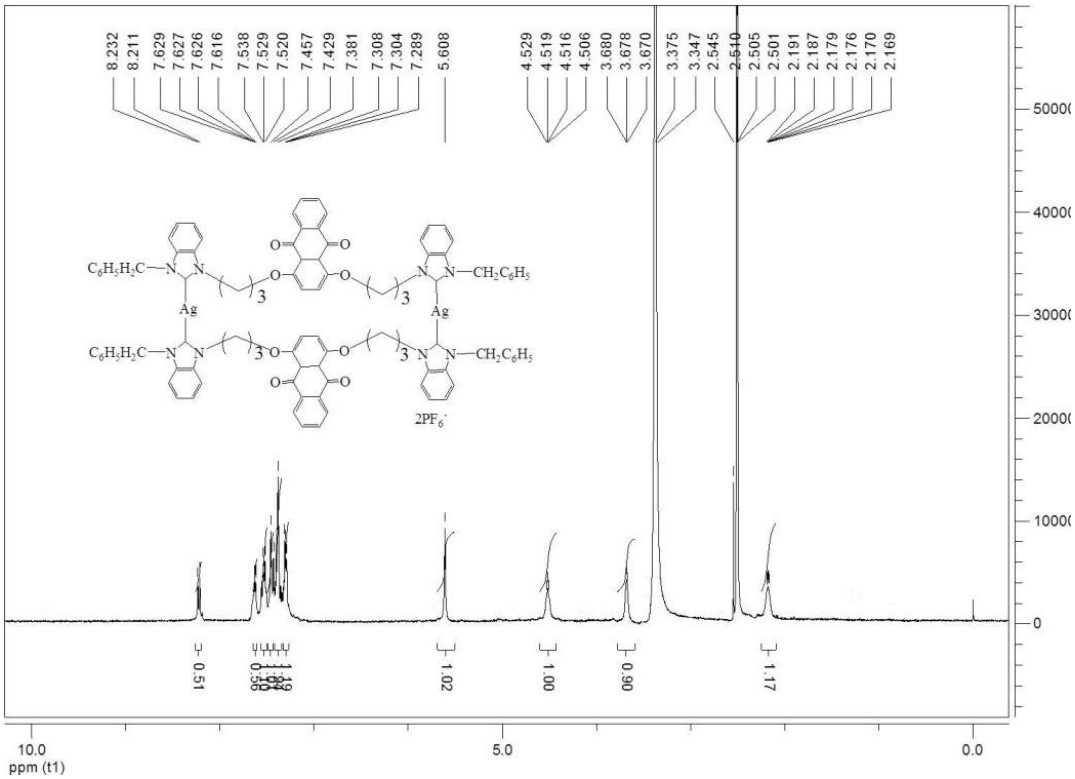

Fig. S26 The ^{1}H NMR (400 MHz, DMSO-d_6) spectrum of complex **3**.

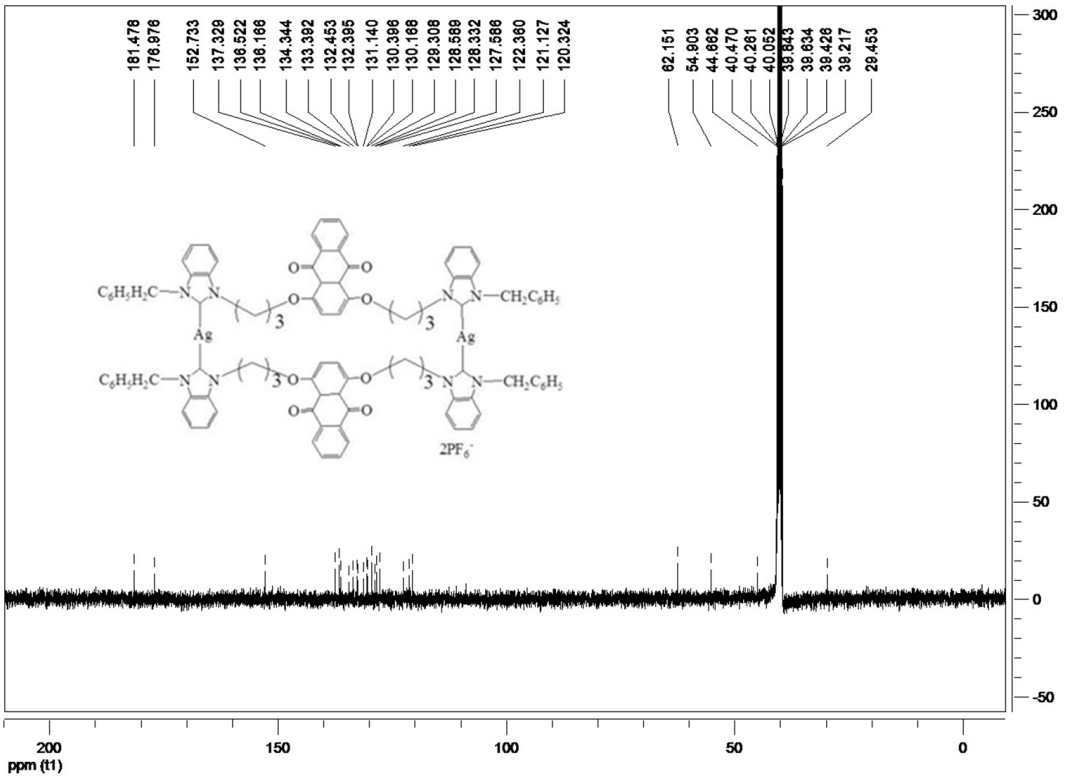

Fig. S27 The ^{13}C NMR (100 MHz, DMSO-d_6) spectrum of complex **3**.

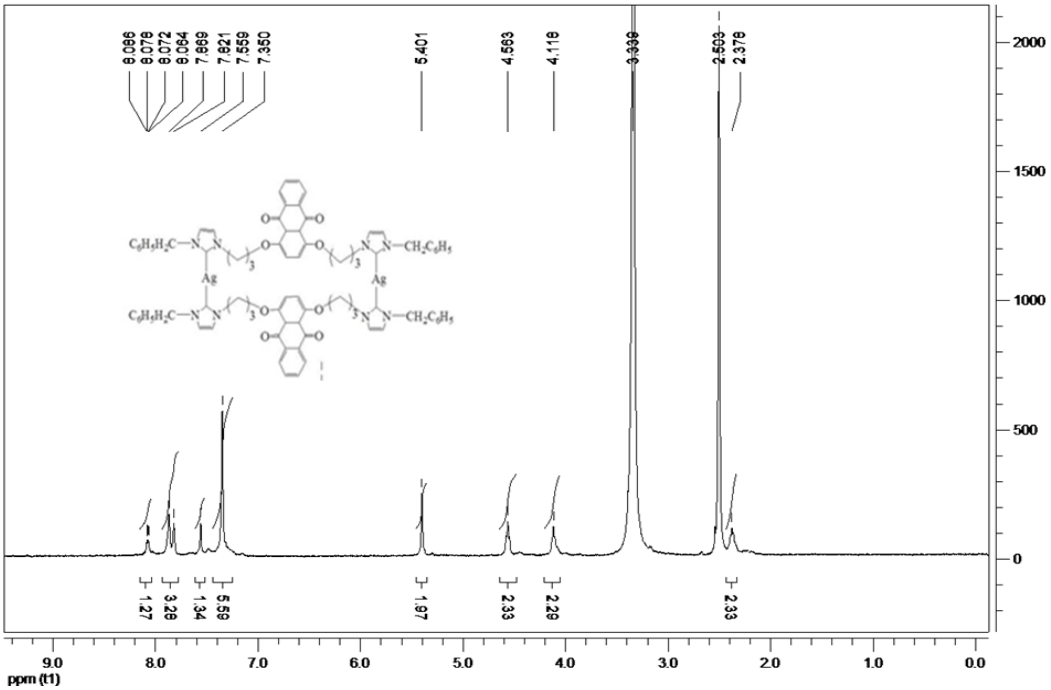

Fig. S28 The ^{1}H NMR (400 MHz, DMSO-d_6) spectrum of complex **4**.

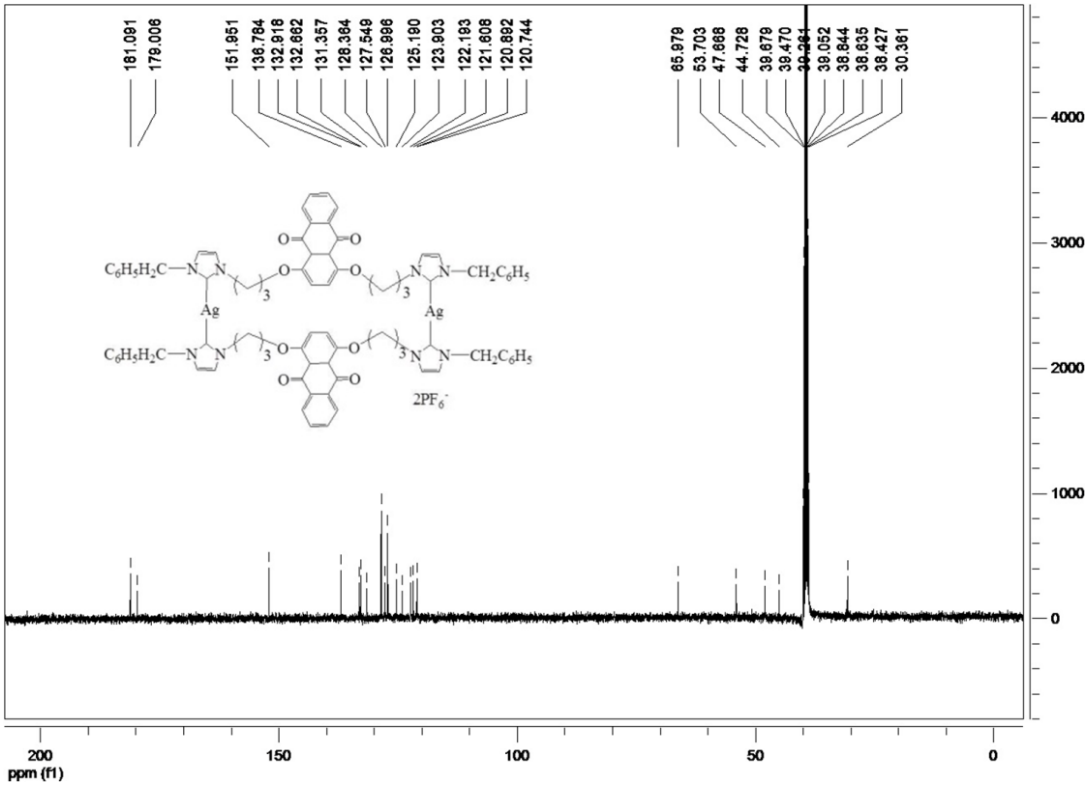

Fig. S29 The ^{13}C NMR (100 MHz, DMSO-d_6) spectrum of complex **4**.